DELPHI Collaboration

DELPHI 2004-013-CONF-689
9 July, 2004

A measurements of the Total Hadronic Cross-section in $\gamma\gamma$ collisions at very low Q^2 at LEP2

S. Almehed [1], **V. Hedberg** [1], **G. Jarlskog** [1], **P. Tyapkin** [1,3], **N. Zimin** [2,3]
[1] Physics Department, University of Lund, Sweden
[2] CERN, Geneva, Switzerland
[3] JINR, Dubna, Russian Federation

Abstract

Results of an experimental study of both single and double tagged events measured in $\gamma\gamma$ collisions are presented. The data have been obtained with the DELPHI detector at LEP2 energies (from 189 up to 206 GeV) with the scattered e^+ and e^- measured by the VSAT detector. A good agreement between data and the full simulation is observed and the total $\gamma\gamma$ hadronic cross-section is estimated for a $\gamma\gamma$ centre of mass energy from 25 to 120 GeV.

Contributed Paper for ICHEP 2004 (Beijing)

1 Introduction

The multihadron production in the reaction $e^+e^- \to e^+e^- + hadrons$ has been studied for the first time at LEP2 energies with one or both scattered electrons (referred to as tags) detected at very low momentum transfer squared, Q^2, by the DELPHI Very Small Angle Tagger (VSAT). Such events are called single or double tagged events depending on the number of detected electrons. Previously, these types of measurements have been performed at lower energies [1–3] and at LEP2 [4, 5] at an intermediate range of Q^2 from data provided by luminosity detectors.

Data collected with the DELPHI detector during 1998-2000, corresponding to an integrated luminosity of 620 pb^{-1}, where hadronic final states were produced in $\gamma\gamma$ collisions were used in the following analysis.

The DELPHI VSAT [6] detector was the principal tool in these studies. It consisted of four identical modules, each with a 3x5 cm^2 active detector area. They were placed symmetrically $\simeq$7.7 m downstream of the DELPHI interaction point behind the superconducting quadrupoles at $\simeq$ 60 mm from the beam line, covering polar angles, θ, between 3-15 mrad. The energy resolution of the VSAT detector was about 4.5% at 100 GeV. It also had a precise measurement of the position of the incoming particles in x and y (about 200 μm), which allowed for an efficient separation of signal from background.

The double tag mode is attractive because the most complete information about the $\gamma\gamma$ process is obtained in this case. From the measured tags, the four-momentum of each virtual photon is known. Thus, in a small angle approximation, a direct reconstruction of the invariant mass, W, of the produced system becomes possible on an event-by-event basis, eliminating the need to infer the W spectrum from the hadrons detected with the use of some unfolding procedure, as it is necessary for no-tag [7] or single-tag events [8]. As a result, a total hadronic cross-section as a function of the $\gamma\gamma$ centre-of-mass energy, W, can be studied with double tag events with significantly smaller systematic errors. In the case of the VSAT detector, where the very low Q^2 range below 0.9 GeV^2/c^4 is covered, the errors coming from the extrapolation of the results to $Q^2 = 0$ are smaller than those obtained in previous experiments. Knowledge of both four-momenta of the tags also permits, in principle, measurements of the interference between photon helicity states [1]. Unfortunately, despite the low angles measured, the number of events are considerably reduced in the double tag case due to the very small acceptance of the modules and the very difficult background conditions which reduce the effective working area of the detectors. In the single tag mode, the available statistics is much larger.

2 The Monte Carlo

According to the current picture, established from studies of hadronic $\gamma\gamma$ processes at e^+ e^- colliders and γp interactions at HERA, a correct description of the experimental data has to use a three-component model: a soft interaction term described by the generalized Vector meson Dominance Model (VDM), a perturbative term described by the Quark Parton Model (QPM) with direct quark exchange, and a term for the hard scattering of the partonic constituents of the photon, the so-called Resolved Photon Contribution (QCD-RPC).

All these models were in one way or another implemented in the three generators used in the present study: TWOGAM (version 2.04) [9], PHOJET (version 1.12) [10] and PYTHIA (version 6.143) [11]. The TWOGAM generator describes DELPHI data

reasonably well as has been shown in previous LEP1 analysis for both the no tag [12] and single tag case [3]. The QPM and VDM events are in the present study generated with the same parameters as in previous DELPHI analyses [12]. The QCD-RPC process was treated by using leading order QCD factorization where a hard scattering subprocess gives the dominant p_T^2 scale, taken also as the factorization scale. Since such subprocesses are considered as perturbative, a single free parameter, p_T^{min}, the transverse momentum of the outgoing partons, has to be specified and used in order to separate the RPC from the non-perturbative contribution. The values of p_T^{min} were found for the parton density functions from the requirement to reproduce the visible experimental two-photon cross-section. The Gordon-Storrow (GS2) parameterization of the parton density functions with $p_T^{min}(GS2) = 2.05(1.88) \pm 0.020\ GeV/c$ has been shown to reproduce the data better than other models and were chosen for the simulation.

The PHOJET generator (version pre-1.12) [10] was created for two-photon physics applications. This version includes an exact photon flux calculation of photon-photon processes in lepton-lepton collisions. The ideas, methods and algorithms used in the program are based on the Dual Parton Model (DPM). In order to combine the DPM, which describes soft processes, with the well-known perturbative QCD, the event generator is constructed as a two-component model (one component for soft and one component for hard processes). Thus, multiple soft and hard interactions may be generated simultaneously since soft and hard processes was treated in a unified way in this program. Hard scattering processes were simulated using lowest-order perturbative QCD. Initial state and final state parton showers were generated in the leading-log approximation. Some coherence effects (angular ordering in the emissions) were taken into account as well. The JETSET 7.4 program was used for the fragmentation of the parton configurations. The GRV parametrization of the parton density function of the photon was used in this analysis. A transverse momentum cutoff, $p_T^{cut} = 2.5\ GeV$, was applied to the partons of the resolved photons to separate soft from hard processes. The program could run only in the hadronic invariant mass region above 5 GeV.

The PYTHIA generator [11] is a general purpose generator in high energy physics since many years but was only recently upgraded to simulate two-photon events. The program uses six event classes for two-photon collisions based on the three-component model of the photon. Version 6.143 has been used in preference to more recent versions because it describes well Deep Inelastic Scattering (DIS) data. In order to use different kinds of events and be free of double counting, the cutoff parameters are introduced at the level of the real photon fluctuation $\gamma \to q\bar{q}$ and the final hadronic system creation $\gamma\gamma^* \to q\bar{q}$. The VDM and anomalous events are together called resolved events. The superposition of events applies separately for each of the two incoming photons and forms six distinct classes of events: direct-direct, VDM-VDM, anomalous-anomalous, direct-VDM, direct-anomalous and VDM-anomalous. In the case of deep inelastic scattering, only one of the photons is resolved and hence only direct-direct, direct-VDM and direct-anomalous components are used in the model. These three contributions are similar to the TWOGAM and PHOJET classifications.

The generated events have been processed by the full detector simulation program and then been subjected to the same selection procedure as the experimental data. A description of the DELPHI detector together with basic criteria used to select tracks and the thresholds applied to neutral particles in the calorimeters can be found in reference [13].

3 The data

The final reprocessed samples with all the corrections applied to individual tracks and neutral particles have been used in the analysis. The scattered electrons were traced backwards in an iterative procedure from the VSAT detector, through the quadrupole and solenoid magnetic fields, to the interaction point by a special program made for VSAT called FASTSIM. The precision of this procedure is best for highly energetic particles that hit the detector close to its center. The accuracy of the angle reconstruction was checked by comparing the reconstructed angles with the generated angles in simulated events.

Studies were made to check the consistency of data samples from different years. The following run-time dependencies were studied and implemented in the reconstruction procedure of the tagged lepton:

- the beam energy (for each LEP fill);
- the leakage corrections (for each beam energy);
- the geometrical position of the VSAT modules (for each year);
- the beam-spot position (for each DELPHI data acquisition run);
- the inclination of the incoming beams (for each DELPHI data acquisition run).

The energy corrections were based on studies of the large sample of Bhabha elastic scattering events with hits covering the full area of the detector modules. The final calibration was done on a fill-by-fill basis correcting the single-arm energy of these events to the beam energy. The other type of corrections is connected to the leakage effect when particles hit the VSAT modules near the edge and some part of the electromagnetic shower escapes from the module. The size of the correction ranges from 0 to 8 GeV, depending on the reconstructed position of the particle. This is one of the largest corrections as can be seen in Table 1.

Correction	Size of corr.	Uncertainty	ϕ (degrees)	θ (mrad)
Energy leakage and calibration	$\approx$ 5 GeV	7%	1°	0.15
Geometrical survey (x,y,z)	$\approx$ 1 mm	200 μm	0.5°	0.07
Off-energy electron position(y)	$\approx$ 1 mm	600 μm	1.5°	0.1
Beam spot correction(x)	$\approx$ 3 mm	20 μm	-	0.03
Beam angle correction in y	$\approx$ 1 mm	$\approx$ 1 mm	2°	0.12
Angle reconstruction	-	-	5°	0.4

Table 1: Corrections applied to the VSAT part of the analyzed events and the resulting uncertainties in ϕ and θ. The beam spot variation have been corrected for in the y and z directions as well. For the beamspot, the effect on θ and ϕ is small, so it has been ignored in this table. The correction of the beam angles is merely a way of treating a shift in angles as a shift in module-position.

The geometrical corrections are intended to fix the geometry of the VSAT with respect to the beams as accurately as possible, in order to be able to reconstruct the angles of the tagged electrons at the vertex with high enough precision. The geometrical survey

measured the position of the VSAT modules with respect to each other with a precision of about 200 μm at the beginning and end of the each yearly data taking period. By studying the sharply peaked impact distribution of the off-momentum electrons in the horizontal-plane, it was possible to align the y-coordinate of the two outer modules with respect to the beam-axis. By further using the strict collinearity of the Bhabha events, the y-coordinate of the two inner modules could also be aligned. The accurate position of the beam spot is as essential to know as the position of the VSAT modules. The angle reconstruction was corrected for the position of the beam-interaction point, as given by the DELPHI beam spot measurements using the central tracking devices on a run-by-run basis. During 1998-2000 the spread in the relative angles of the beams was less than 100 μrads. The effect this had on the VSAT measurements corresponded to approximately 0.3 mm variations in the measured y-coordinate. This variation was treated by shifting the VSAT modules on a fill-by-fill basis, in order to align the y-position by using the off-momentum electrons and Bhabha events as described above. In this way the shift due to the beam tilt at the interaction point was translated into a correction of the position of the VSAT. The resulting error on the reconstructed angles is thus the same as before the operation, but the result is easier to compare to a simulation, where different beam-angles are not implemented.

Extensive studies were performed to eliminate the off-momentum electron background as much as possible, as an efficient rejection of the background is one of the major problems in this type of analysis. Independent studies performed by the CERN SL Division [14] at the DELPHI interaction point demonstrated that background conditions at LEP2 were much worse than those at LEP1. Using the LEP luminosity monitors they found that the background event rate normalized to the Bhabha events almost doubled when the energy increased up to 91.5 GeV. Later, during the last year of LEP operations (2000), the background was even higher. The main source of background came from random coincidences between two independent events incorrectly recorded as the same, i.e., the showers detected by the VSAT modules were not coming from the same process as the hadronic system detected by the main DELPHI detector.

When $\gamma\gamma$ events are studied in single tag mode, only one electron/positron is measured. The main background source to that process is the coincidence between an off-energy electron/positron and a no-tag $\gamma\gamma$ event.

For double-tagged $\gamma\gamma$ events, the background came mainly from three sources, i.e., when there were coincidences between:

a) a normal Bhabha event measured by VSAT and a hadronic activity from an un-tagged $\gamma\gamma$ event;

b) two off-momentum electrons hitting VSAT modules on opposite sides, again with hadronic activity from no-tag $\gamma\gamma$ events;

c) one off-momentum electron hitting a VSAT module while a scattered electron was hitting the opposite VSAT module (single tagged $\gamma\gamma$ event).

All these sources of background have different intrinsic features and they had to be treated separately.

In order to reject Bhabha events in the analysis, a set of cuts on the tagged electrons were applied to the data. These cuts were customized to eliminate the Bhabha background as efficiently as possible, thereby taking advantage of the strict collinearity of this elastic scattering process. Extensive studies of Bhabha events, revealed that they were confined to a narrow region in the plane of δX and δY, where δX denotes the difference in the measured X coordinates of the two electrons and δY similarly refers to the Y coordinates. For the true double tagged two-photon events the two quantities show significantly broader distributions than the Bhabha events. A cut on the two quantities was applied corresponding to 2σ of the measured Bhabha distribution. Events within this region and with a measured energy in the VSAT of more than 70% of the beam energy were marked as Bhabha events and rejected. The cut was applied on a fill-by-fill basis, since the quantities fluctuate with the specific beam-conditions. A cut on the total event energy was also applied, since any Bhabha event superimposed on a two photon event, will result in a higher energy than the beam-energy. The cut was set at 115 GeV.

Studies of Bhabha events showed that the δX and δY cuts, as described above, rejected 90% of the Bhabha background while the true two-photon events were not affected. The cut on total energy rejected 93% of the remaining background, while again the true two-photon events were not affected. It was thus possible to reduce the background by 99.3%, without losing any signal events.

The off-momentum background in the VSAT modules depended on the beam spot positions and the beam's inclination angles. The background (especially its high energy component) was concentrated in certain areas of the two dimensional plot showing the Y position as a function of the energy. A typical distribution of off-energy electrons in the Y-E plane is shown in Fig. 1. One can see from the plot that a trivial mathematical expression cannot be used to describe the background region and for this reason two-dimensional cut-maps were used.

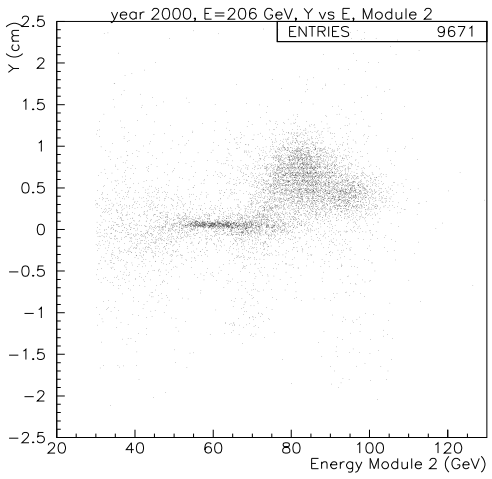

Figure 1: The VSAT high energy background distribution in the Y-E plane for VSAT module 2 for one fill during 1999.

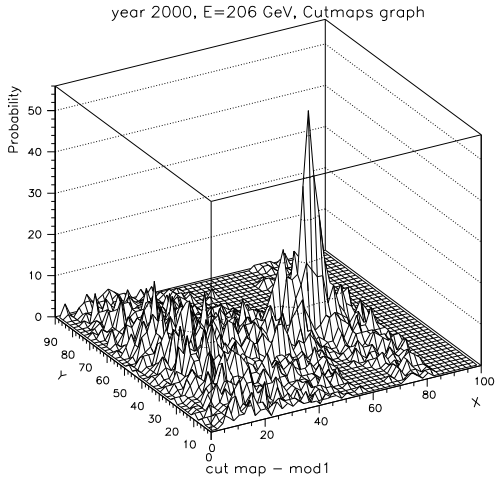

Figure 2: The probability of having a background event as a function of the energy (shown as X) and the Y position of the hit. The probability is given in units of permill.

The primary source of information used in constructing the cut-maps came from off-energy electron background events recorded by other DELPHI triggers. Due to the fact that the background usually changed both in size and position with changes of the LEP parameters, the cut-maps were created for each module and LEP energy (see Fig. 2).

The transformed variables $Y_{map} = (y - y_0 + 1.6) \cdot 25 + 1$ and $X_{map} = E_{beam} - E + 11$ were used for that. Here E_{beam} is the beam energy, y_0 is the average Y-position (in cm) of the off-energy background for each DELPHI run while Y and E are the Y-position (in cm) and energy (in GeV) of the measured electron. If the Y_{map} or X_{map} variable was outside the map border, the event was accepted. The probability of having a background electron in each bin was calculated and defined a third coordinate Z. The cut used was therefore a cut-off value in the horizontal plane in Fig. 2. All events above the cut-limit were rejected by the cut. The cut-limits were set differently for different modules (inner modules, for example, always had lower limits than the outer modules) and energy regions.

4 Data - Monte Carlo comparison

The final samples of two-photon events were prepared by a sequential selection procedure. The first step was to separate single from double tag events by the number of modules that were hit. For tag particles the following was required:

- the correctness of the X and Y position measurement;
- that the energy measured by the VSAT module was above 30 GeV;
- that the second electron was not seen in the experiment in the single tag case. It was therefore required that the energy of each individual particle was below 30 GeV (25 GeV for neutral particles) in the whole DELPHI detector;
- that the double tag events had passed the Bhabha rejection criteria;
- that the electrons had fulfilled the cut-map selection.

For particles in the $\gamma\gamma$ hadronic system the following selection criteria were applied:

- $4 \leq N_{Charged} \leq 18$ for single tag event and $3 \leq N_{Charged} \leq 18$ for double tag event for charged tracks which had a momentum of at least 0.3 GeV and were found in the angular region $10^o \leq \theta \leq 90^o$;
- the total energy of the hadronic system should be less than 45 GeV;
- the transverse momentum should be less than 5 GeV;
- the minimal invariant mass of the hadronic system should be larger than 3 GeV.

After all rejection and selection criteria were applied the residual background was found to be $\simeq$12% in the final $\gamma\gamma$ sample of single tag events and about 35% in the double tag events sample. It was subtracted from the data in the final step.

An identical selection procedure was used also in the selection of the simulated double and single tagged events.

The numbers of events and corresponding luminosities for real data and simulated samples are given in Tables 2.

Sample	Luminosity pb^{-1}	E_{cms} GeV	Recorded/simulated number of events	Single tag selected	Double tag selected
1998 year					
Data	146.2	189	86624	4763	103
TWOGAM	300.0	189	52311	8669	347
PHOJET	411.0	189	84554	19263	784
PYTHIA	512.8	188.6	113929	23191	576
1999 year					
Data	29.0	192	17523		
	82.4	196	49734	Total	Total
	76.0	200	45856	2355	127
	32.6	202	19688		
TWOGAM	450.0	200	90784	15178	245
PYTHIA	552.6	199.5	123039	27796	705
2000 year					
Data	153.1	206	84024	4608	93
TWOGAM	450.0	206	92133	15107	330
PHOJET	382.1	206	80419	20269	412
PYTHIA	494.3	206.5	108929	28902	591

Table 2: The number of events and the luminosity in the data and the simulated samples.

The normalization to the data luminosity was done for all simulated samples. The number of events produced by the generators for each year were then multiplied by a factor to get the number of simulated events equal to the number of events in the corresponding data sample. This was done so one could better compare the shape of the distributions from the different simulations with each other and with real data.

The renormalization factors for the TWOGAM single tag sample were close to one: 0.90 - 1.10 (depending on the year). PHOJET and PYTHIA both tended to overestimate the number of single tag events and needed renormalization factors from 0.47 to 0.58 for PHOJET and from 0.52 to 0.72 for PYTHIA. A similar situation was observed for the double tag case: the renormalization factor for TWOGAM was 1.0, for PHOJET it was 0.6 and it was 0.7 for PYHTIA.

The renormalized plots of the scattered positron energy as measured by VSAT are shown in Fig. 3 and Fig. 4. The background in the outer modules (1 and 3) was much higher than in the inner modules (2 and 4) and the cut-map requirement therefore distorted more the energy distribution in the outer modules. This is the reason why only events tagged by the inner modules were used in the total hadronic cross-section calculations.

Comparisons have also been made for three VSAT energy regions (30-60 , 60-90 and 90-120 GeV) between the generated and reconstructed Monte Carlo samples.

The relative difference between E_{gen} and E_{rec} i.e. $(E_{gen} - E_{rec})/E_{rec}$, was in all cases less than 3% with an RMS less than 6%. This showed that the energy measurement by VSAT was not biased by the reconstruction procedure.

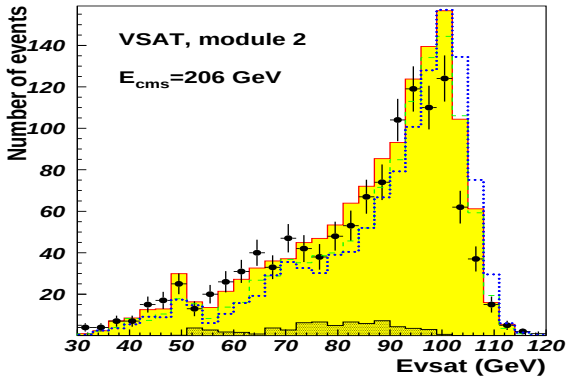

Figure 3: The energy distribution measured by module 2 of VSAT in year 2000. The points are data, TWOGAM is shown as a solid line and a shaded area, PHOJET as a dashed line and PYTHIA as a dotted line. The hatched dark area is the subtracted background.

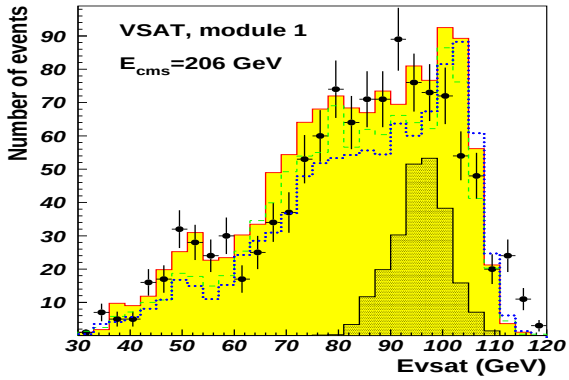

Figure 4: The energy distribution measured by module 1 of VSAT in year 2000. The points are data, TWOGAM is shown as a solid line and a shaded area, PHOJET as a dashed line and PYTHIA as a dotted line. The hatched dark area is the subtracted background.

After all corrections and the background rejection procedure were applied, the samples from different years were compared. All the distributions were found to be consistent with each other. The combined distributions of the single tag events for all years are shown in Fig. 5 - 7. They were compared and found to be in a reasonable agreement with the simulation. The subtracted background is shown in all distribution as hatched dark areas. The distribution of energy in VSAT relative to the beam energy (Fig. 5 a) shows a good agreement between data and simulation. Some disagreements with the simulated distributions is visible around the peak. The multiplicity distributions of particles in the hadronic system, as measured by the barrel and forward detectors of DELPHI, are also in a good agreement with the predictions of all generators, except in the low multiplicity region as shown in Fig. 5 b.

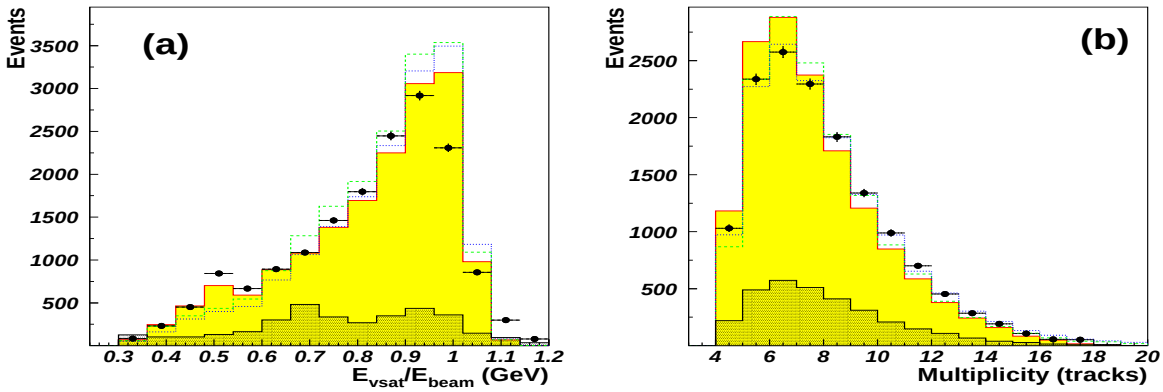

Figure 5: Comparison of data and normalized Monte Carlo for single-tag events: a) The relative energy of scattered e^+ and e^- measured in VSAT, b) The event multiplicity. Points are data, hatched area is the background, lines show Monte Carlo: solid line and shaded area is TWOGAM, the dashed line is PHOJET and the dotted line is PYTHIA.

Previously, an unfolding procedure [15] has been used as a tool to reconstruct a so-called "true" invariant hadronic mass (W_{inv}). In spite of the fact that it has been reconsidered and reevaluated recently with the appearance of the LEP II data and the new event generators, the unfolding procedure has many inherent problems mainly due to the different final topologies for the VDM, QPM and BCD-RPC type of $\gamma\gamma$ events [16].

All this means that it is not prudent to assume that the unfolding results are model independent. For this reason a simplified calculation of the W_{inv} variable was introduced in this analysis. After a Monte Carlo study of different correlations between the "true" W_{inv} and other variables, a fenomenological formula was derived that was found to be giving a good estimation of the "true" invariant mass in the simulated samples:

$$W_{inv} = K_0 \cdot (E_{Beam} - E_{VSAT}) + K_1 \cdot W_{Had} \pm K_2 \cdot (\theta_{Had} - 90^o)/10^o \qquad (1)$$

where $\pm$ before the last element $(\theta_{Had} - 90^o)/10^o$ must be positive for forward modules (1 and 2) and negative for backward modules (3 and 4). K_0, K_1, K_2 are the coefficients which were adjusted (to 1.0 - 1.1, 2.0 - 2.4, 1.2 - 1.4 respectively) so that the generated invariant mass W_{inv}^{gen} could be reconstructed from the measured variables such as hadronic invariant mass W_{Had} (invariant hadronic mass measured by DELPHI barrel detectors) and θ_{Had} (the resulting azimuthal angle of the total momentum of the particles detected in the barrel).

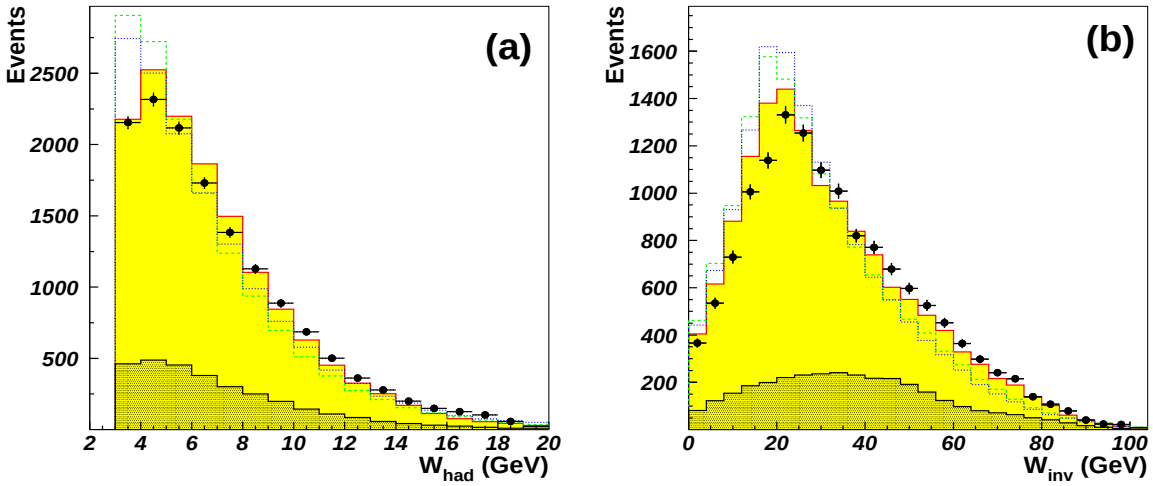

Figure 6: Comparison of single tag data and normalized Monte Carlo events: a) The invariant mass of the hadronic system, b) Reconstructed invariant mass. Points are data, the hatched area is the background, lines show Monte Carlo: solid line and shaded area is TWOGAM, the dashed line is PHOJET, and the dotted line is PYTHIA.

The TWOGAM program seems to give a wider W_{inv} distribution (see Fig. 6 b) which agrees better with data than the PHOJET and PYTHIA generators. All of the generators seems to be shifted to lower values of the invariant mass in comparison with data.

The distribution of the transverse momentum of the hadronic system in Fig. 7 b shows that all generators disagree somewhat with the data for a P_t below 1 GeV. There is also some disagreement between the Q^2-distribution in Fig 7 a.

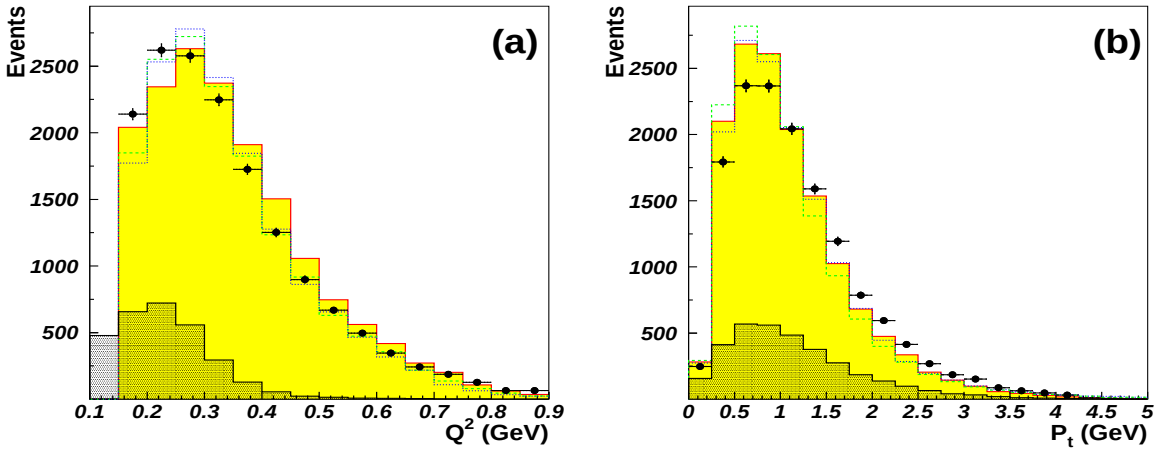

Figure 7: Comparison of data and normalized Monte Carlo for single-tag events: a) The distribution of Q^2, b) The transverse momentum of the hadronic system. Points are data, the hatched area is the background, lines show Monte Carlo: solid line and shaded area is TWOGAM, the dashed line is PHOJET, and the dotted line is PYTHIA.

The background rejection in the double tag analysis is based on the same cut-maps as for the single tag events with the averaged purity estimated to be 83%.

Data and the Monte Carlo predictions for double tag events are shown in Fig. 8, 9 and 10 and agree within the statistical errors.

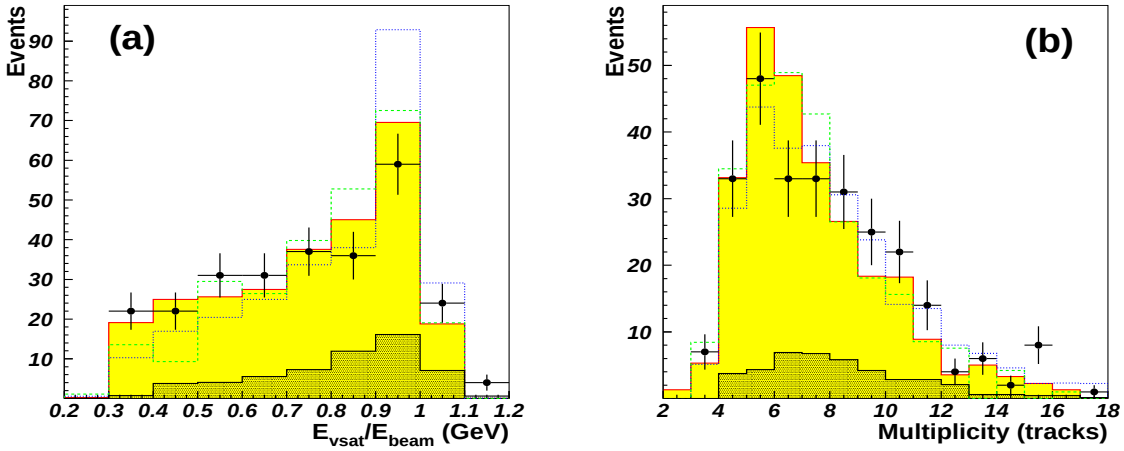

Figure 8: Comparison of data and normalized Monte Carlo for double tag events: a) The relative energy of scattered e^+ and e^- measured in VSAT, b) The event multiplicity. Points are data, the hatched area is the background, lines show Monte Carlo: solid line and shaded area is TWOGAM, the dashed line is PHOJET, and the dotted line is PYTHIA.

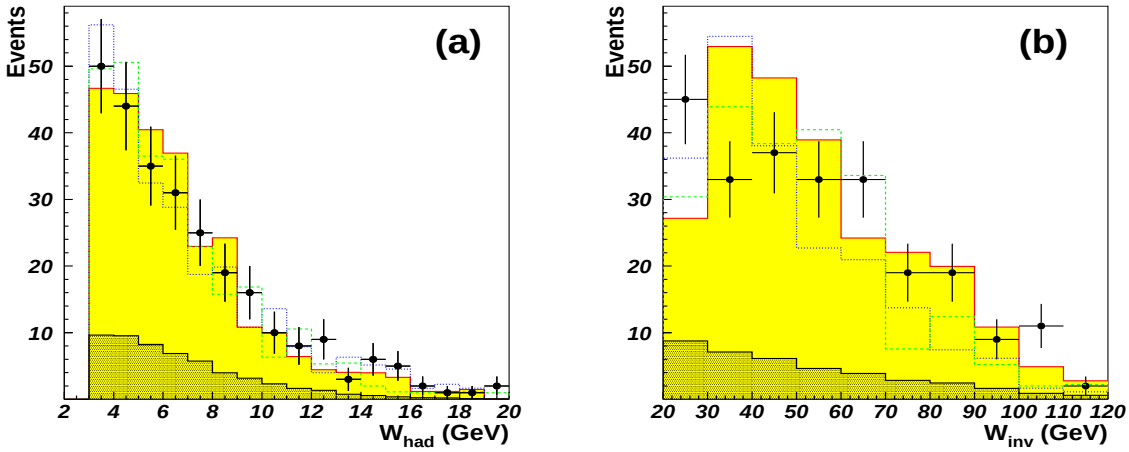

Figure 9: Comparison of data and normalized Monte Carlo for double tag events: a) The invariant mass of the hadronic system, b) Reconstructed invariant mass. Points are data, the hatched area is the background, lines show Monte Carlo: solid line and shaded area is TWOGAM, the dashed line is PHOJET, and the dotted line is PYTHIA.

It seems that all generators work better when both particles have a scattering angle far from zero in contrast to the events with very low Q^2 (which is impossible to reach if both leptons are tagged). For such events there is an indication that the simulation disagree increasingly with a decreasing Q^2. Therefore the differences between data and simulated samples are larger in the single tag case.

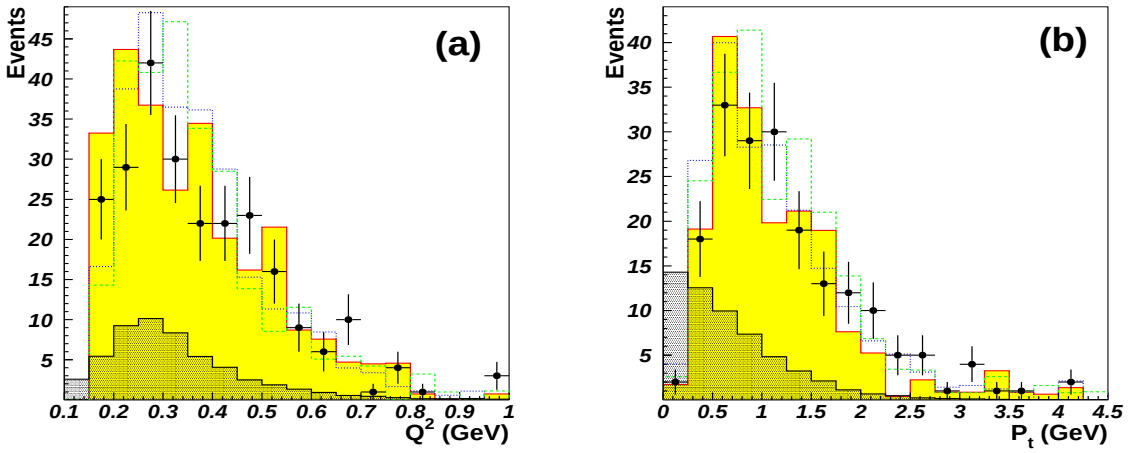

Figure 10: Comparison of data and normalized Monte Carlo for double tag events: a) The distribution of Q^2, b) The transversal momentum of hadronic system. Points are data, the hatched area is the background, lines show Monte Carlo: solid line and shaded area is TWOGAM, the dashed line is PHOJET, and the dotted line is PYTHIA.

5 Cross-section calculation

In order to extract the total $\gamma\gamma$ cross-section it is necessary to calculate the luminosity function of the photon flux. A considerable improvement to the equivalent photon approximation [17] for two-photon production was recently made in a work by Schuler [18], in which the previously used forms of the equivalent photon approximation were critically examined. The improved calculation of the two-photon luminosity function which includes beyond-leading-logarithm effects is implemented into the GALUGA program [19], used to calculate the photon flux for both the single tag and double tag topologies. An example of such a calculation for the single tag case is shown in Fig. 11. These luminosity functions (and similar ones for double tag events) were used in the extraction of the total $\gamma\gamma$ cross-section.

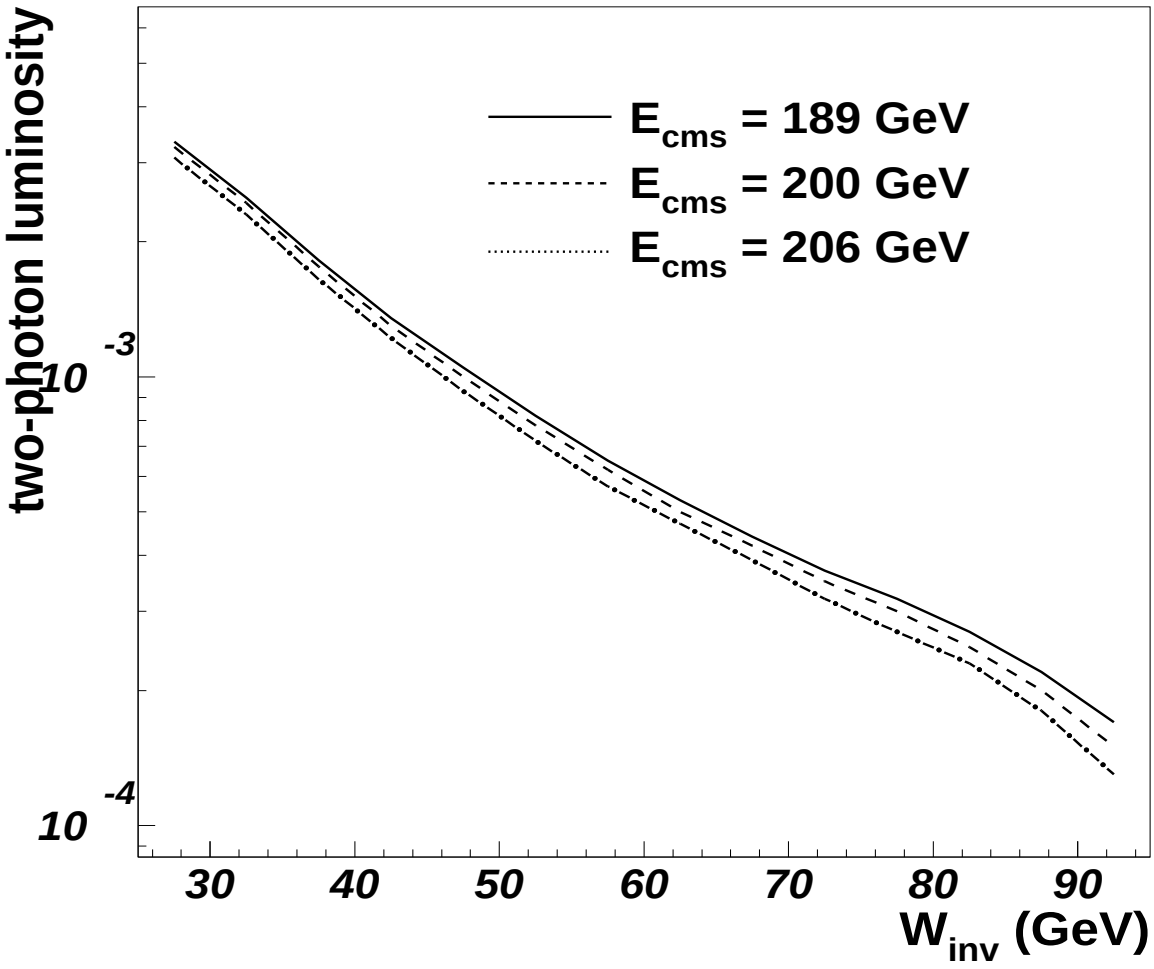

Figure 11: The two-photon luminosity function versus W_{inv} for different beam energies (189 GeV is shown as a dash-dotted line, 200 GeV as a dashed line and 206 GeV as a solid line). The so-called "two-photon luminosity" is the probability to have a $\gamma\gamma$ interaction.

Another very important task, in order to get the total $\gamma\gamma$ cross-section extracted correctly, is the transformation from the effective cross-section $e^+e^- \to hadrons$ measured in the experiment to the real cross-section of this physics process.

The level of complexity of this problem is clearly shown in Fig. 12 and 13 where the generated invariant mass distributions are shown for all generated events and those that passed all the selection criteria. Both the single and double tag distributions can be seen in comparison with the initial distribution of the generated W_{inv} in Fig. 12 and then after selection in Fig. 13. Due to the small acceptance of the VSAT detector (including the cut-maps in the background subtraction procedure) the selection of events introduces a drastic change in the shape of the distribution of the reconstructed W_{inv}.

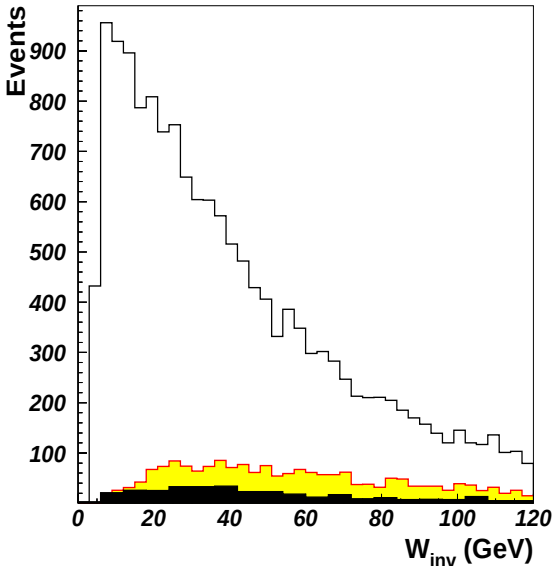

Figure 12: The simulated W_{inv} distribution (module 2) of year 2000 data. The solid line is W_{inv} before selection. After single tag selection is shown as a shaded area. The dark area is the selected double tag events in all modules.

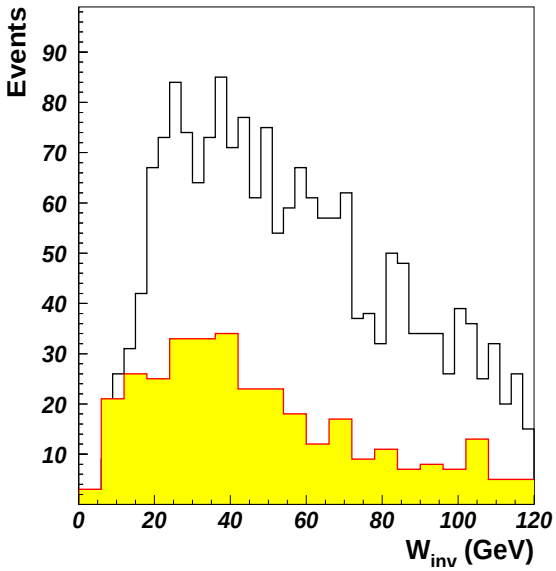

Figure 13: The simulated W_{inv} distribution after the selection of single tag events (module 2) and of double tag events (all modules) for year 2000. The solid line is for single tag data while double tag is shown as a shaded area.

Since the simulated samples agree well with data (after renormalization of TWOGAM, PYTHIA and PHOJET) all of them have been used to calculate the detection efficiency at different invariant masses of the hadronic states and with all effects of the event selection included. An efficiency averaged over all simulated samples was finally used in the total $\gamma\gamma$ cross-section calculations. Specially generated samples with TWOGAM for no-tag conditions were used to transform the cross-section in single and double tag topologies to the total effective $\gamma\gamma$ cross-section of the process $\gamma\gamma \to hadrons$. This was done for the same W_{inv} intervals that were used in the extraction.

As the inner VSAT modules were considerably less affected by the background conditions, only events tagged by those modules have been used for the cross-section extraction in the single tag case in the 6 intervals of invariant mass. Final results are given in Table 3.

W_{inv}, GeV	30-36	36-42	42-50	50-60	60-75	75-100
Data	1071	815	901	803	672	267
TWOGAM	1514	1222	1227	1228	1222	1010
PHOJET	2472	1851	1883	1621	1203	473
PYTHIA	2769	2055	1800	1575	1184	531
Statistical error, %	3.1	3.5	3.3	3.5	3.9	6.1
Systematical error, %	2.6	2.7	2.7	2.8	2.9	3.3
Total error, %	4.0	4.4	4.3	4.5	4.9	7.0
σ_{tot}, nb	370	406	437	474	513	604
Statistical error, nb	11	15	15	17	20	37
Systematical error, nb	10	11	12	13	15	20
Total error, nb	15	18	19	21	25	42

Table 3: The numbers of real events in different samples and the effective $\gamma\gamma$ hadronic cross-section for single tag events. The total error was calculated as the quadratic sum of the statistical and systematical error.

The average contributions to the systematic errors from different sources were estimated as follows:

- the background rejection procedure: $\sim 2.0\%$;
- the event selection procedure: $\sim 0.9\%$;
- the generation of no-tag samples: $\leq 0.7\%$;
- the calculation of the photon luminosity function: $\leq 0.2\%$.

The uncertainties due to the limited Monte-Carlo statistics used in the determination of the detection efficiency in different invariant mass intervals are also included in the systematic errors. The systematic error (calculated as the quadratic sum of the individual systematic errors) is therefore different for different W_{inv} intervals. The total errors shown in Table 3 are also calculated as the sums in quadrature of the statistical and systematical errors.

The total effective $\gamma\gamma$ cross-section was extracted in the same fashion from the double tag events. Due to the lower statistics, the event sample was only split into 4 intervals of invariant mass. All four VSAT modules were used as tagging devices. Thus both the diagonal (inner and outer modules) and the parallel (inner-inner or outer-outer) combinations contributed to the final data sample. Final results for the double tag case are shown in Table 4.

W_{inv}, GeV	20-34	34-50	50-72	72-100
Data	89	76	77	81
TWOGAM	310	238	208	266
PHOJET	256	208	176	92
PYTHIA	574	302	238	148
Statistical error, %	10.6	11.5	11.4	11.1
Systematical error,%	5.4	6.0	6.4	7.2
Total error, %	11.9	13.0	13.1	13.2
σ_{tot}, nb	344	412	478	624
Statistical error	36.5	47.4	54.5	69.3
Systematical error	18.6	24.7	30.6	44.9
Total error, nb	41	54	63	83

Table 4: The numbers of real events in different samples and the effective $\gamma\gamma$ hadronic cross-section for double tag events. The total error was calculated as the quadratic sum of the statistical and systematical error.

The systematic errors were estimated in the same manner as in the single tag analysis. For each W_{inv} interval the averaged uncertainties were as follows:

- the background rejection procedure: $\sim 4.0\%$;
- the event selection procedure: $\sim 1.0\%$;
- the generation of no-tag samples: $\leq 0.7\%$;
- the calculation of the photon luminosity function: $\leq 0.2\%$.

Analogously to the single tag case, these systematic errors are different for each W_{inv} interval, since the Monte Carlo statistics used in the determination of the detection efficiency varied between W_{inv} intervals.

The total $\gamma\gamma$ cross-section for both the single and double tag case is shown in Fig. 14 together with a compilation of measurements from L3 and OPAL. The total $\gamma\gamma$ cross-section predicted by the TWOGAM generator is also shown.

The DELPHI measurements seem to be somewhat higher than what has been observed by L3 [4] and OPAL [5].

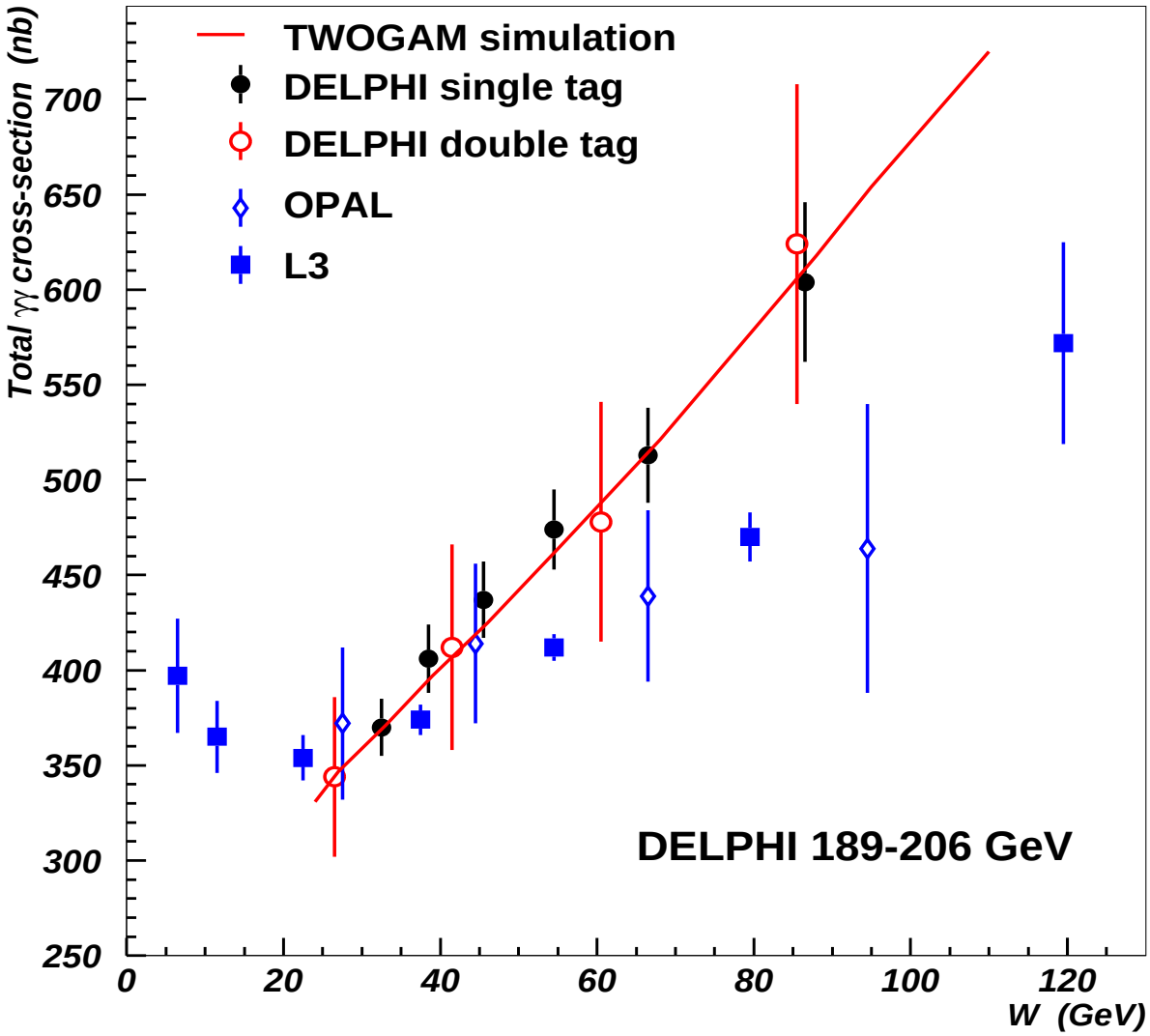

Figure 14: The total hadronic $\gamma\gamma$ cross-section measured by VSAT for single tag events (filled circles), double tag (open circles), TWOGAM simulation results (line), results from OPAL (open rombs) and L3 (filled rectangles). The error bars represents the total error.

The statistical uncertainty in the new VSAT double tag measurement is considerably smaller than in a previous work [20] based on a small sample of VSAT double tag events but it is consistent with it. The errors from the VSAT single tag events are of course noticeably smaller than those of the double tag events due to the better statistics. Results from all experiments indicate an approximately linear rise of the cross-section as a function of the invariant mass of the hadronic system. This can be explained by the predicted rise of the RPC process.

6 Conclusions

Hadronic events produced in two-photon collisions in single and double tag mode at centre-of-mass energies $\sqrt{s} \simeq$ 189 - 206 GeV have been studied. Different experimental distributions can be reproduced by the simulation with reasonable accuracy. An effective total $\gamma\gamma$ cross-section have been measured in a $\gamma\gamma$ centre-of-mass energy range up to 100 GeV and for events with very low Q^2 (much closer to Q^2=0 than what has been studied by other LEP experiments). The rise of the $\gamma\gamma$ cross-section with W seen in this study is somewhat steeper than in previous measurements by the L3 [4] and OPAL [5] collaborations.

References

[1] TPC/2γ Coll., D. Bintinger et al., *Phys. Rev. Lett.* **54** (1985) 763.

[2] DELPHI Coll., P. Abreu et al., *Phys. Lett.* **B342** (1995) 402.

[3] N. Zimin, Proceedings of the Photon '97: the XIth International Workshop on Gamma-Gamma Collisions: Egmond aan Zee, The Netherlands, 10-15 May, 1997.

[4] M. Acciarri et al. (The L3 Collaboration),
Total Cross Section measurement in $\gamma\gamma$ Collisions at LEP 2.
CERN-EP/2001-012, January 30, 2001

[5] OPAL Coll., K. Ackerstaff et al., Eur. Phys. J. **C 14** (2000) 199.

[6] S.Almehed et al., Nucl.Inst. and Meth. **A305**(1991) 320.

[7] Ch. Berger et al., *Phys. Lett.* **B99** (1981) 287.
TPC/2γ Coll., *Phys. Rev.* **D41** (1990) 2661.

[8] DELPHI Coll., P. Abreu et al., *Phys. Lett.* **B342**(1995) 402. TPC/2γ (1985) 763.

[9] Physics at LEP2, Editors: G.Altarelli, T. Sjöstrand, F. Zwinger
CERN 96-1, Geneva, 1996, Vol.2, p. 224.
S. Nova, A. Olshevski and T. Todorov, DELPHI Note 90-35(1990).

[10] R. Engel, Z. Phys. **C66** (1993) 1657;
R. Engel and J. Ranft, Hadronic photon-photon interactions at high energies, ENSLAPP-A-540/95, September 1995.

[11] T. Sjöstrand, Comput. Phys. Comm. **82** (1994) 74;
PYTHIA 5.7 and JETSET 7.4: Physics and manual,
preprint CERN-TH 7112/93-REV.

[12] DELPHI Coll., P. Abreu et al., *Z. Phys. C - Particles and Fields* **62** (1994) 357.

[13] DELPHI Coll., P. Abreu et al., *Nucl. Instrum. Methods* **A378** (1996) 57.

[14] E. Bravin, B. Dehning, G.P. Ferri, A. Forsstrom, M. Merkel,
Luminosity measurements at LEP., CERN-SL-97-72 (BI)

[15] V. Blobel, In Proceedings of the CERN School of Computing,
Aiguablava, Spain, (1984), CERN 85-09.

[16] I. Tyapkin. Study of the hadronic photon structure function with the DELPHI detector at LEP. PHOTON 2001 Conf. Proc., Ascona, Switzerland.

[17] V.M. Budnev, I.F. Ginzburg, G.V. Meledin and V.G. Serbo,
Physics Reports (Section C of Physics Letters) 15, no. 4 (1975)181-282.

[18] G.A. Schuler, CERN-TH/96-297 (1996).
Improving the equivalent-photon approximation in electron-positron collisions.

[19] Gerhard A. Schuler. Two-photon physics with GALUGA 2.0.
Computer Physics Communications 108 (1998) 279-303.

[20] Andreas Nygren. Hadronic Structure Measurements of the Photon by DELPHI at LEP II. Lund University doctoral dissertation: LUNFD6(NFFL-7199)2001.
ISBN 91-628-4932-8